The facile one-step hydrothermal method to prepare MnO_2 nanoparticles: Structural and electrochemical properties

K Tangphanit[1], N Boonraksa[1], S Maensiri[2], E Swatsitang[3] and K Wongsaprom[1,*]

[1]Department of Physics, Faculty of Science, Mahasarakham University, Mahasarakham, 44150, Thailand
[2]School of Physics, Institute of Science, Suranaree University of Technology, Nakhon Ratchasima, 30000, Thailand
[3]Institute of Nanomaterials Research and Innovation for Energy (IN-RIE), NANOTEC-KKU RNN on Nanomaterials Research and Innovation for Energy, Khon Kaen University, Khon Kaen, 40002, Thailand

*E-mail: kwanruthai.w@msu.ac.th

Abstract. MnO_2 nanoparticles were successfully prepared via one-step hydrothermal method. The surface are properties of the MnO_2 nanoparticles were determined by BET nitrogen adsorption-desorption measurement. The XRD analyses confirm the pure phase of γ-MnO_2 and α-MnO_2, having orthorhombic crystal structure (JCPDS file no.14-0644 and 44-0141). FE-SEM analysis reveals the combination of massively small spherical particles with average particle size 54.8 nm. The electrochemical results revealed that the MnO_2 nanoparticles delivered the specific capacitance of 200.83 F/g at a current density of 1A/g. The cycle stability was usability 30% after 500 cycles at a current density of 5 A/g. The MnO_2 nanoparticles reveal a energy density of 3.62 Wh/kg under a power density of 43.11 W/kg.

1. Introduction

Current demand for energy is increasing, due to the energy crisis and global warming. This is to explore novel materials for advanced energy storage devices. Supercapacitors are the most promising candidates for advanced energy storage devices because of its excellent properties such as long cycle life, high power density and fast charge-discharge rate [1, 2]. One main objective for studying in this field is to explore novel material with high capacitance and fast charging [3]. The transition metal oxides (viz. NiO, Co_2O_3, TiO_2, RuO_2, MnO_2, Fe_2O_3, etc) [4-9] have been demonstrated as novel electrode materials for pseudocapacitors. Among these oxides, MnO_2 is prominent as it reveals excellent electrochemical behaviour which are widely used in applications [10-12]. It is well-known that the surface structure strongly influence the electrochemical behaviour. The different synthesis methods are enhanced the electrochemical properties of electrode materials. One of synthesis method to prepare electrode materials with various morphology and low cost is hydrothermal techniques. Xiao *et al.* [13] reported the sample of α-MnO_2 with a high capacitance 220 F/g at 5 mV/s in 0.1M Na_2SO_4 electrolyte solution prepared by the hydrothermal method. Moreover, different shape of MnO_2 reveal good capacitance of 317, 204 and 276 F/g at 5 mV/s for nanospheres, hollow urchins and smooth balls, respectively [14].

We herein present the structural and electrochemical properties of MnO_2 nanoparticles synthesized by the one-step hydrothermal method. X-ray diffraction (XRD) was used to determine the structure of

the MnO_2 nanoparticles. The morphological analysis was investigated by field emission scanning electron microscopy (FE-SEM). Energy dispersive X-ray spectrometer (EDS) was used to characterize the chemical composition of the nanoparticles. The pore size analysis of the MnO_2 nanoparticles was studied using Brunauer-Emmett-Teller (BET) method. The electrochemical performance was examined by cyclic voltammetry (CV) and galvanostatic charge-discharge (GCD).

2. Experimental procedure

Nanoparticles of MnO_2 were prepared by the one-step hydrothermal method. Manganese nitrate [Mn $(NO_3)_2.6H_2O$] and potassium permanganate [$KMnO_4$] were dissolved and stirred in 100 mL of deionized water (DI water) at ambient temperature. The solution was changed to a Teflon-lined stainless-steel autoclave, sealed and maintained at 180 ˚C for 3 h. After the autoclave was cooled naturally to ambient temperature, the product was washed several times with DI water and ethanol separately. Then the product was dried in vacuum oven at 70 ˚C for 24 h. The structural analysis of the MnO_2 nanoparticles was investigated by XRD (Bruker-D8 advanced X-ray diffractometer). The shape and elements of the sample were examined by FE-SEM and EDS, respectively. The porous nature of the MnO_2 nanoparticles were performed using BET method. The electrochemical properties were examined by CV and GCD.

3. Results and discussion

Figure 1 presents the XRD pattern of the MnO_2 sample. The XRD pattern shows the diffraction corresponded to the γ-MnO_2 phase (JCPDS No.14-0644) with the orthorhombic structure. Moreover, the α-MnO_2 phase was also observed (JCPDS No.44-0141) and consistent with the research of Zhang *et al.* [15]. The peaks of impurity phases of Mn, Mn_2O_3 or Mn_3O_4 are not observed in the sample.

The elemental composition of MnO_2 nanoparticles was determined by EDS as presented in figure 2. The sample reveals peaks of Mn and O, no evidence of impurity phases, the presence of Au came from Au coated on the sample. The shape of the MnO_2 sample was studied by FE-SEM as shown in the inset of figure 2. FE-SEM image shows the small spherical particles of a uniform particle size. Moreover, these platelets are densely overlapped and aggregated. The average particle size is approximately 54.8 nm. The aggregation of particles was caused by the short reaction time of the hydrothermal process, consistent with the research of Wang *et al.* [16] synthesized a spherical α-MnO_2 using the hydrothermal method.

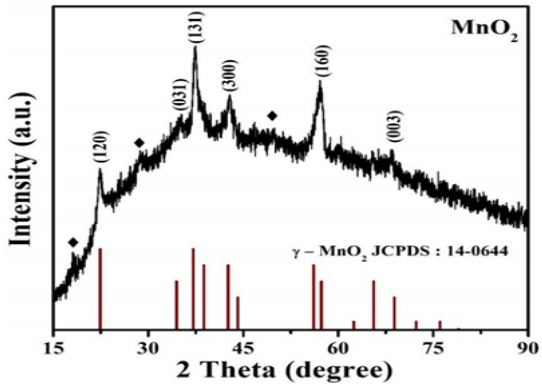

Figure 1. XRD pattern of MnO_2 nanoparticles, ♦ represents the phase of α-MnO_2.

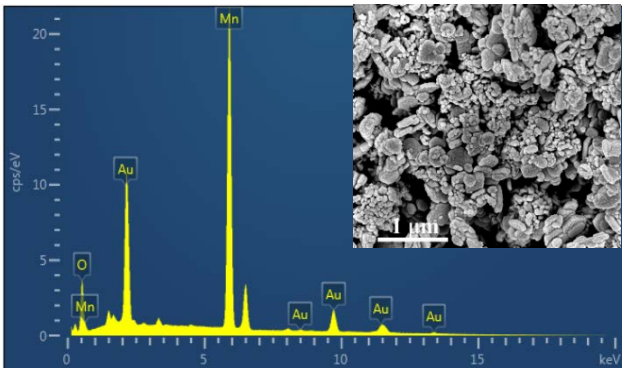

Figure 2. EDS spectrum and the inset shows the FE-SEM image of MnO_2 nanoparticles.

We investigated the specific surface area and pore size of the MnO_2 nanoparticles via nitrogen adsorption-desorption measurement. The result revealed the III Type isotherm, according to IUPAC classification as presented in figure 3. The calculation of pore size distribution was studied by the BJH (Barrett-Joyner-Halenda) method [inset in figure 3]. The pore volume and average pore diameter of the

sample are 0.30 cm^3/g and 3.30 nm. The specific surface area is 7.01 m^2/g, which calculated by BET. According to the obtained structure of MnO_2 and those of low specific surface area, pore volume and pore diameter, this could result in a low specific capacity value.

The capacitive properties of the MnO_2 sample were examined by CV analysis. CV curves of the sample within the scan range 2 to 200 mV/s in a potential range -1 to 0.55 V are shown in figure 4. The CV curves show the pseudocapacitive behaviour of the sample, anodic peak appearing at 0.0 to 0.2 V and the cathodic peak shows two peaks at 0.2 and -0.3 to -0.4 V. The occurrence of more than one reaction in an intercalation / deintercalation process of the MnO_2 ion group follows the equation [17, 18].

$$MnO_2 + OH^- \rightarrow MnOOH + e^- \quad (1)$$

$$MnOOH + e^- \rightarrow HMnO_2 + e^- \quad (2)$$

$$MnOOH + HMnO_2^- \rightarrow Mn_3O_4 + H_2O + OH \quad (3)$$

From these reactions, it can be seen that the oxidation number of Mn has been changed from Mn^{4+} to Mn^{3+} and Mn^{2+}, during the reaction of the electrolyte and the electrode material. As a result, the electrode resistance and reaction resistance are increased. This result is agree with the study of Kaiyu *et al.* [18]. The increase in resistance could result in a lower specific capacitance value.

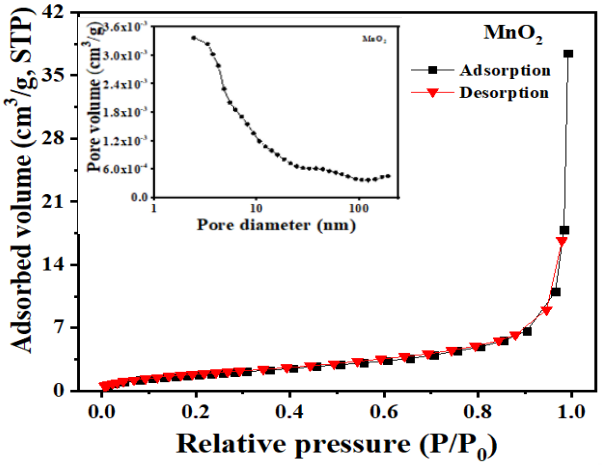

Figure 3. Nitrogen adsorption-desorption isotherms of MnO_2 nanoparticles.

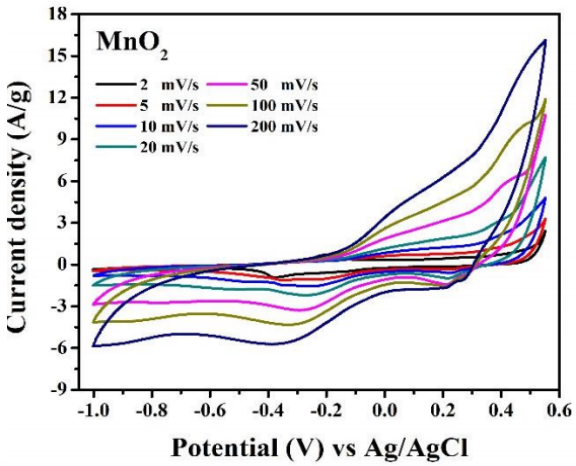

Figure 4. CV curves of the MnO_2 nanoparticles.

The electrochemical performance of the sample was further evaluated by GCD analysis as shown in figure 5. The sample electrode have three levels of discharge at different current densities. The first level is in a potential range -0.1 to 0.55V, the second level is in a potential range -0.5 to -0.1V and the third level is in a potential range 0.6 to -1V. The discharge is due to the change in the oxidation number of MnO_2, according to the reversible redox-reaction [19]. The specific capacitance is 200.83 F/g at a current density of 1 A/g. Figure 6 presents the cycle stability of sample with a usability of 30% after 500 cycles of charge and discharge at a current density of 5 A/g. The sample revealed an energy density of 3.62 Wh/kg under a power density of 43.11 W/kg. This low specific capacitance is due to the spherical shape of MnO_2, resulting in less contact area. In addition, it has a low pore diameter and pore volume.

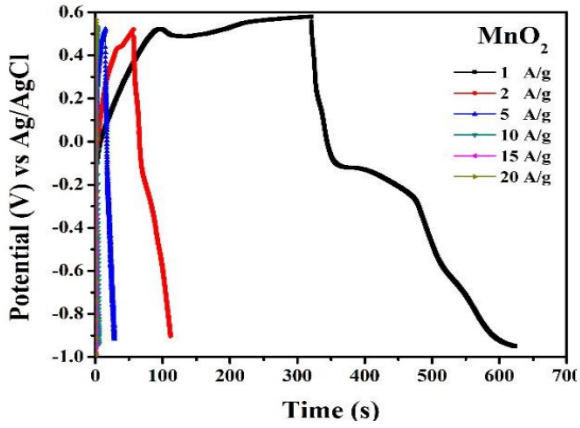

Figure 5. GCD curves of the MnO_2 nanoparticles.

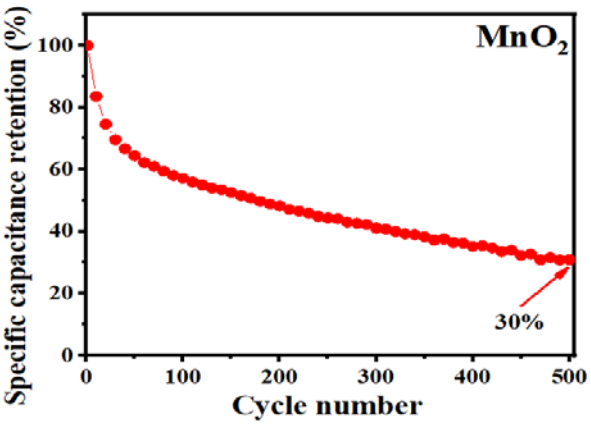

Figure 6. The cycle stability of MnO_2 sample at 5 A/g.

4. Conclusion

The MnO_2 sample was prepared by the one-step hydrothermal method. Pure phase of γ-MnO_2 and α-MnO_2 are detected in the structures. The average particle size is approximately 54.8 nm. More than one reaction occurred at the MnO_2 electrode resulting from a change in the oxidation numbers of Mn^{4+} to Mn^{3+} and Mn^{2+} ions. The MnO_2 nanoparticles showed a good specific capacitance of 200.83 F/g with 30% retention after 500 cycles. This research may be useful for further development of oxide synthesis techniques for fabrication of electrode materials.

Acknowledgments

The authors would like to thank the center of excellence in advanced functional materials, Suranaree University of Technology, Thailand for CV and GCD facilities. This work was financially supported by Thailand Science Research and Innovation (TSRI) 2021.

References

[1] Poonguzhali R, Shanmugam N, Gobi R, Senthikumar A, Viruthagiri G and Kannadasan N 2015 *J. Power Sources* **293** 790
[2] Ramirez-Castro C, Crosnier O, Athouël L, Retoux R, Bélanger D and Brousse T 2015 *J. Electrochem. Soc.* **162** A5179
[3] Wei C, Pang H, Zhang B, Lu Q, Liang S and Gao F 2019 *Sci. Rep.* **3** 2193
[4] Kim S-I, Lee J-S, Ahn H-J, Song H-K and Jang J-H 2013 *ACS Appl. Mater. Interfaces* **5** 1596
[5] Jayalakshmi M and Balasubramanian K 2008 *Int. J. Electrochem. Sci.* **3** 1196
[6] Lu X, Wang G, Zhai T, Yu M, Gan J, Tong Y and Li Y 2012 *Nano Lett.* **12** 1690
[7] Jiang Q, Kurra N, Alhabeb M, Gogotsi Y and Alshareef H N 2018 *Adv. Energy Mater.* **8** 1703043
[8] Kulal P M, Dubal D P, Lokhande C D and Fulari V J 2011 *J. Alloys Compd.* **509** 2567
[9] Xia A, Yu W, Yi J, Tan G, Ren H and Liu C 2019 *J. Electroanal. Chem.* **839** 25
[10] Ghodbane O, Pascal J L and Favier F 2009 *ACS Appl. Mater. Interfaces* **1** 1130
[11] Ray A, Roy A, Saha S, Ghosh M, Chowdhury S R, Maiyalagan T, Bhattacharya S K and Das S 2019 *Langmuir* **35** 8257
[12] Simon P and Gogotsi Y 2008 *Nat. Mater.* **7** 845
[13] Xiao W, Xia H, Fuh J Y H and Lu L 2009 *J. Power Sources* **193** 935
[14] Li N, Zhu X, Zhang C, Lai L, Jiang R and Zhu J 2017 *J. Alloys. Compd.* **692** 26
[15] Zhang Y, Li G Y, Lv Y, Wang L Z, Zhang A Q, Song Y H and Huang B L 2011 *Int. J. Hydrog Energy* **36** 11760
[16] Wang F, Zhou Q, Li G and Wang Q 2017 *J. Alloys. Compd.* **700** 185

[17] Jayachandran M, Rose A, Maiyalagan T and Vijayakumar T 2021 *Electrochim. Acta* **366** 137412
[18] Kaiyu L, Ying Z, Wei Z, He Z and Geng S 2007 *Trans. Nonferrous Met. Soc. China* **17** 649
[19] Kate R S, Khalate S A and Deokate R J 2018 *J. Alloys Compd.* **734** 89